Spin-flip exchange scattering of low-energy electrons in ferromagnetic iron

M. Plihal
Department of Physics and Astronomy, Rutgers University, Piscataway, New Jersey 08855

D. L. Mills
Department of Physics and Astronomy, University of California Irvine, Irvine, California 92697
(Received 20 May 1998)

We present a theory of spin-flip exchange scattering of low-energy electrons, directed at the ferromagnetic transition metals, with application to Fe. The model used employs a tight-binding description of the paramagnetic spd bands. Ferromagnetic exchange splitting of the bands is achieved by including on-site Coulomb repulsion between electrons in $3d$ orbitals, which is treated in a mean-field approximation. The low-energy electron interacts with the metal electrons via the Coulomb interaction, and the magnetic excitations in the metal are treated within the random-phase approximation. Both spin waves and Stoner excitations contribute to the energy loss of the low-energy electron. We show that the relative importance of these two loss mechanisms is influenced very importantly by the degree of localization of the $3d$ orbital. We also present results based on the use of accurate wave functions. These show that spin-wave loss peaks should be prominent features in spin-polarized electron energy-loss spectra. [S0163-1829(98)03745-X]

I. INTRODUCTION

In itinerant electron ferromagnets such as Fe, Co, or Ni, there are two classes of magnetic excitations. One has low-lying collective excitations, the spin waves. In addition, there is a continuum of particle-hole excitations in which the spin of the electron is flipped. These are referred to commonly as Stoner excitations.

There have been remarkably few experimental studies of the magnetic excitations in the classic materials just mentioned, particularly at large wave vectors where our recent theoretical studies[1] show the spin-wave spectrum to be remarkably sensitive to details of the electronic band structure, at least in ferromagnetic Fe. Neutron scattering has been employed to study spin-wave excitations, but in a material such as Fe, the spin-wave exchange stiffness is so large one cannot explore them beyond 25% of the way from the Brillouin-zone center, to the zone boundary. Through use of a spallation source, Perring *et al.*[2] have explored aspects of the excitation spectra of Fe at large wave vectors, though the data are limited. It is striking to us that so little is known about the magnetic excitations of this well-known ferromagnet.

Electron energy-loss spectroscopy (EELS), or its spin-polarized version (SPEELS) offers the possibility of probing magnetic excitations in such materials, over a wide range of energy and wave vector. Here the incident electron has energy which may range from 20 eV to a few hundred electron volts. In this energy range, the electrons have very short mean free paths, so electron loss spectroscopy proves a powerful probe of excitations at surfaces, and in ultrathin films. Experiments which use spin-polarized electron beams, and spin detectors can isolate contributions to the loss spectrum in which the spin of the beam electron is flipped. Such ''complete experiments'' have explored Stoner excitations in Fe and other magnetically ordered metals.[3,4] However the much lower energy spin waves have yet to be detected since the experiments to date have energy resolution insufficient to address these features. An earlier estimate of the cross section,[5] based on a simple model, and the calculations presented in the present paper suggest one should be able to observe these modes, with presently available spectrometers.

We comment next on the issue which motivates the calculations here. First, the ability to interpret SPEELS spectra in more than a qualitative manner has been inhibited by the absence of quantitative theory for real materials. Activity in the field has declined as a consequence, in our view. This has stimulated theoretical efforts to generate a quantitative theory of the loss spectra; the theory of the magnetic excitations in itinerant ferromagnets is, of course, a central issue. While very substantial efforts have been devoted to the study of ground-state properties of magnetic surfaces and ultrathin films,[6] very little has been directed toward their excitation spectra. Our recent paper[1] is a publication which addresses such questions, within the framework of a model based on a realistic electronic structure.

One must also develop a description of the scattering process itself. Within the framework of a relativistic multiple-scattering theory, this issue was addressed recently.[5] The physical picture which underlies the scattering event is that the beam electron sees an array of spins disordered by fluctuations, and is deflected away from the specular or Bragg directions by an inelastic event in which energy is exchanged with the fluctuations. It was assumed in Ref. 5 that as the substrate moments fluctuate, they do so as rigid entities, unchanged in magnitude and shape. A consequence is that the SPEELS spectrum is described by the wave-vector and frequency-dependent transverse spin susceptibility $\chi_{+-}(\vec{q},\omega)$ encountered frequently in discussions of the response of magnetic materials to external probes.[7] We have recently completed detailed studies of $\chi_{+-}(\vec{q},\omega)$ for bulk Fe, and its counterpart for ultrathin films of Fe.[1] Spin waves, broadened by Landau damping, appear as strong features as

they have in earlier theoretical studies of bulk Fe.[8] However, the Stoner excitations appear only as very weak features in this response function, while they show most clearly in the experimental SPEELS spectra. If we combine the formalism of Ref. 5 with the results for $\chi_{+-}(\vec{q},\omega)$ in Ref. 1, the predicted Stoner spectrum is far too weak. We remark that in the bulk, in the limit $\vec{q}\rightarrow 0$, considerations of spin rotation invariance requires the Stoner contribution to vanish identically. We have found that even at large values of $\vec{q}$, it is surprisingly weak.

In this paper, we address the issue of the origin of the strong Stoner contributions to SPEELS spectra, with the intention of providing a quantitative theory of the strength of the spin-wave feature relative to the Stoner continuum. In physical terms the assumption in Ref. 5 that the substrate moments rotate rigidly as they participate in the thermal fluctuations must be reexamined. As they fluctuate, we must take due account of the fact that they change shape and magnitude. Stated otherwise, we require a more realistic exchange matrix element to couple the beam electron to the spin excitations.

We may see that this is so from an earlier study of spin-flip electron scattering put forth by Vignale and Singwi.[11] These authors present a theory of SPEELS in bulk itinerant ferromagnets within the framework of a very simple picture of the electronic structure of the substrate. They address neutron scattering as well. The electrons all reside in parabolic energy bands, with wave functions of plane wave form. A phenomenological, rigid exchange splitting is introduced for substrate electrons. The neutrons couple to the substrate through $\chi_{+-}(\vec{q},\omega)$, in their picture, while use of a microscopic exchange matrix element in the descriptions of SPEELS leads to a more complex response function. In their studies of the neutron spectra, one sees the Stoner spectrum is indeed weak compared to the spin-wave features as in our recent studies, while it is strong in the SPEELS calculations. In their model, for high beam electron energy, the expression for the SPEELS cross section becomes proportional to $\chi_{+-}(\vec{q},\omega)$, with the consequence that the Stoner spectrum weakens relative to the spin-wave portion at high impact energy.

As we discussed earlier[1] and mentioned above, the weak Stoner structure in $\chi_{+-}(\vec{q},\omega)$ has its origin in a fundamental theorem. Spin-rotation invariance requires that as $\vec{q}\rightarrow 0$, all the oscillation strength resides in the spin-wave pole at $\omega = 0$. Evidently, as we see from the work of Vignale and Singwi[11] and our recent studies, even at large wave vectors the Stoner spectrum remains weak. No such theorem applies to the response function that is relevant when a full microscopic exchange matrix element is employed.

The theoretical situation in the theory of SPEELS thus differs substantially from that of phonon losses in electron-energy-loss spectra. In the latter case, theories based on the notion that the potential of an ion shifts rigidly when the nucleus is displaced provide very quantitative accounts of the measured loss spectra.[12]

In the present paper, we develop a description of a microscopically based exchange matrix element suitable for the calculation of SPEELS spectra, when an empirical tight-binding description of the substrate band structure is employed. We then explore SPEELS spectra for spin-flip electron scattering in bulk Fe, to find strong Stoner contributions. Use of this matrix element allows us to generate quantitative SPEELS spectra, for model descriptions in which the electronic band structure is realistic. We find, as discussed below, that the ratio of the spin wave to Stoner strength is sensitive to the nature of the wave functions employed for the substrate electrons. We illustrate this with model calculations. Our final set of studies employs realistic wave functions, for the case of Fe, and provides us with accurate estimates.

Our interest ultimately resides in a realistic study of the SPEELS spectra of ultrathin films of Fe. All calculations presented here explore the losses experienced by a plane-wave ''hot electron'' in bulk Fe. The theory for the ultrathin film is under development presently.

II. THEORETICAL MODEL

In our previous paper,[1] our theoretical analysis of the dynamic spin susceptibility of bulk Fe, and of ultrathin Fe films, was based on a model of electronic structure provided by the empirical Slater-Koster parametrization scheme. One associates five $3d$ Wannier orbitals with each lattice site, along with three $4p$ and one $4s$ orbital. Empirical values for the various hopping integrals between first through second neighbors are chosen to reproduce energy bands of paramagnetic Fe generated by *ab initio* calculations. We employed values from the literature, and developed a multiband extension of the Hubbard model to describe the intra-atomic Coulomb interactions which produce ferromagnetism. In our picture, electrons interact when they reside within the $3d$ orbitals associated with one particular lattice site. We have three adjustable parameters in this picture of the Coulomb interaction; these are chosen to reproduce features of the ferromagnetic ground state of Fe. Full details are given in Ref. 1.

Within this scheme, we do not need explicit forms of the wave functions of the electrons, to explore the dynamic spin susceptibility. These are, in fact, form factors of wave functions which enter, but we find the results rather insensitive to their precise form, so long as one takes care to endow the model forms with proper symmetry. Thus, in the results reported in Ref. 1, we employed rather crude models of the form factors.

For reasons outlined in Sec. I, to calculate realistic SPEELS spectra, we require explicit forms for the wave functions of the valence electrons of the ferromagnetic metal. As we shall demonstrate, the results are sensitive to the spatial structure of the Wannier functions used in the evaluation of the exchange matrix element. In this section, we discuss our form for the matrix element, along with our means of generating the SPEELS spectrum once this is in hand.

To begin our discussion, we illustrate the basic exchange scattering process in Fig. 1(a). We imagine a beam electron, or ''hot electron'' with momentum $\vec{p}_i$ and spin down. It engages in a Coulomb scattering with a valence electron of spin up, wave vector $\vec{k}$, and which resides in energy band n. The valence electron is excited to state $\vec{p}_f\uparrow$, and becomes the final-state electron in this exchange scattering, while the electron $\vec{p}_i\downarrow$ is deexcited into an empty minority-spin state.

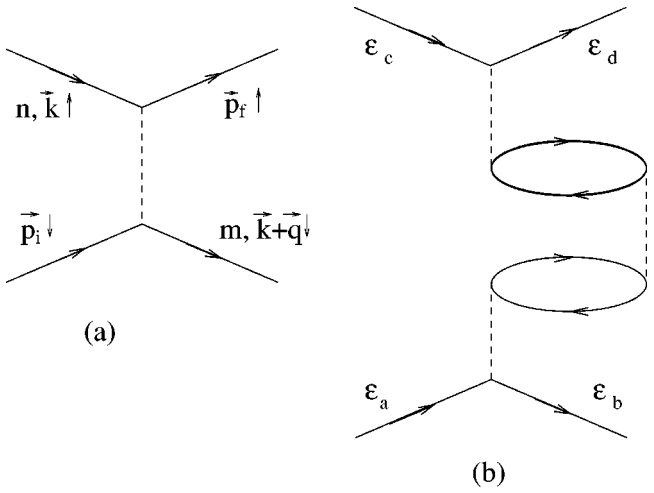

FIG. 1. (a) The basic spin-flip exchange scattering process explored in this paper. Here $(\vec{p}_i\uparrow)$ and $(\vec{p}_f\downarrow)$ are the initial and final-state beam electron, while $(n\vec{k}\uparrow)$ and $(m\vec{k}+\vec{q}\downarrow)$ reside in the valence bands of the ferromagnetic host. (b) A schematic illustration of the diagrams which contribute to the screening of the process delineated in (a).

In the end, we have spin-flip scattering of the beam electron from state $\vec{p}_i$ to state $\vec{p}_f$.

The beam electron will be described by a wave function that is a simple plane wave. The Bloch function associated with the substrate electron is written

$$\psi_{n\vec{k}\sigma}(\vec{x})=\sum_{\mu\vec{R}} a_\mu(n\vec{k}\sigma)e^{i\vec{k}\cdot\vec{R}}\phi_\mu(\vec{x}-\vec{R}). \tag{1}$$

Functions $\phi_\mu(\vec{x}-\vec{R})$ are normalized so the integral of their square over all space is unity. We are interested in excitations of the d-electron system, so in the sum over μ, we retain five d orbitals $\phi_\mu(\vec{r}-\vec{R})$; two have e_g character, and three have t_g character. The admixture coefficients $a_\mu(n\vec{k}\sigma)$ are generated from the empirical band-structure scheme discussed above. We shall require explicit forms for the orbitals $\phi_\mu(\vec{r}-\vec{R})$ in what follows. We write

$$\phi_\mu(\vec{\rho})=R_2(\rho)\sum_m A_{\mu m}Y_{2m}(\hat{\rho}), \tag{2}$$

where $A_{\mu m}$ is the transformation matrix from the spherical harmonics basis to the basis of $\{e_g,t_{2g}\}$ orbitals. Our choice of $R_2(\rho)$ is discussed below.

A. Description of the exchange scattering process

We can imagine the beam electron encounters the substrate in an initial state $|M\rangle$, and excites it to a final state $|N\rangle$, through the process depicted in Fig. 1(a). We describe this by introducing a scattering amplitude we write as

$$A_{\vec{p}_i\downarrow,n\vec{k}\uparrow\to\vec{p}_f\uparrow,m\vec{k}+\vec{q}\downarrow}=\sum_{n,m,k} V^*_{\rm ex}(n\vec{k}\uparrow,\vec{p}_i,\vec{p}_f,m\vec{k}+\vec{q}\downarrow)\times\langle N|c^+_{m\vec{k}+\vec{q}\downarrow}c_{n\vec{k}\uparrow}|M\rangle. \tag{3}$$

The exchange matrix element in Eq. (3) is given by

$$V_{\rm ex}(n\vec{k}\uparrow,\vec{p}_i,\vec{p}_f,m\vec{k}+\vec{q}\downarrow)=\int d^3x\int d^3y\,\psi^*_{n\vec{k}\uparrow}(\vec{x})e^{-i\vec{p}_i\cdot\vec{y}}\times v(|x-y|)e^{i\vec{p}_f\cdot\vec{x}}\psi_{m\vec{k}+\vec{q}\downarrow}(\vec{y}). \tag{4}$$

In this expression, $v(|x-y|)$ is the electron-electron interaction. The form of this interaction appropriate to the present analysis is discussed shortly.

It will be convenient to introduce operators which describe the act of particle-hole creation, weighted by suitable exchange matrix elements associated with each pair. Thus, we define

$$R^+(\vec{q},\vec{p}_i)=\sum_{n_1n_2\vec{k}} V^*(n_1\vec{k}+\vec{q}\downarrow\vec{p}_f;\vec{p}_in_2\vec{k}\uparrow)\times c^+(n_2\vec{k}\uparrow)c(n_1\vec{k}+\vec{q}\downarrow). \tag{5}$$

The operator $R^-(\vec{q},\vec{p}_i)$ is the Hermitian conjugate of $R^+(\vec{q},\vec{p}_i)$. Central to our analysis will be a two-particle Green's function formed from these operators. We define

$$G(\vec{q},\vec{p}_i;\tau)=-\langle T_\tau\{R^+(\vec{q},\vec{p}_i;\tau)R^-(-\vec{q},\vec{p}_i;0)\}\rangle, \tag{6}$$

where T_τ is the time ordering operator on a complex time contour.

Through use of the scattering amplitude defined in Eq. (3), it is a standard matter to derive the cross section $(d^2\sigma/d\omega d\Omega)$ where $(d^2\sigma/d\omega d\Omega)d\omega d\Omega$ is the probability the incident electron is scattered into solid angle $d\Omega$, with energy loss between $\hbar\omega$ and $\hbar(\omega+d\omega)$, accompanied by a spin flip. We omit details here, since by now such derivations are standard. We find

$$\frac{d^2\sigma}{d\omega d\Omega}=-\frac{V^2}{4\pi^2}\frac{m^2}{\hbar^4}\frac{p_f}{p_i}\frac{1}{e^{\beta\omega}-1}\,\mathrm{Im}\,\chi(\vec{q}\vec{p}_i;\omega), \tag{7}$$

where

$$\chi(\vec{q}\vec{p}_i;\omega)=\int dt e^{i\omega t}G^R(\vec{q}\vec{p}_i;t) \tag{8}$$

and $G^R(\vec{q}\vec{p}_i;t)$ is the retarded real-time Green's function associated with that defined in Eq. (6). We remind the reader that, with our convention, the spectral density is negative, and thus, of course, the cross section is positive.

As mentioned in Sec. I, the earlier theory of SPEELS[5] assumed that the beam electron scattered inelastically from magnetic moments in each unit cell which rotate as rigid entities, as they participate in magnetic fluctuations. This earlier analysis incorporated a full multiple-scattering description of the beam electron's propagation through the crystal. If we apply the description of the inelastic event given in Ref. 5 to the plane-wave electron considered presently, the inelastic cross section would be given by an expression virtually identical to Eq. (7), but with one very crucial difference. In place of $\mathrm{Im}\,\chi(\vec{q}\vec{p}_i;\omega)$ we will have the spectral density associated with transverse fluctuations of spin density of wave vector $\vec{q}$. That is, let $S_+(\vec{x},t)=S_x(\vec{x},t)+iS_y(\vec{x},t)$ be the second quantized operator which describes the spin density in the d electron at time t, with $S_-(\vec{x},t)$ its Hermitian adjoint. Upon taking the Fourier trans-

form of these objects, one forms $S_+(\vec{q},t)$ and $S_-(\vec{q},t)$. Within our Bloch representation, suppressing explicit reference to the time t, we have

$$S_+(\vec{q})=\sum_{nm\vec{k}} c^+(n\vec{k}\uparrow)c(m\vec{k}+\vec{q}\uparrow)\langle n\vec{k}\uparrow|e^{-i\vec{q}\cdot\vec{x}}|m\vec{k}+\vec{q}\downarrow\rangle. \tag{9}$$

The two-particle propagator form from $S_+(\vec{q},t)$ and $S_-(\vec{q},t)$ analogous to Eq. (6) is the dynamic transverse susceptibility $\chi_{+-}(\vec{q},t)$. In previous work, we presented detailed studies of the spectral density of this function for bulk Fe, and the associated generalization for ultrathin Fe films. We found a prominent spin-wave feature in these spectral densities for both cases, but there was very little integrated strength in the Stoner region of the spectrum even at large wave vectors. The Stoner excitations show clearly in the experimental data.[3,4]

We argued earlier[1] that the weak Stoner contribution to $\chi_{+-}(\vec{q},t)$ is a consequence of spin-rotation invariance in the Hamiltonian, for the following reason. In the bulk material, and at $\vec{q}=0$, spin-rotation invariance requires all the oscillator strength in the spectral density to reside in the spin-wave pole, which is at $\omega=0$ in this limit. The Stoner spectrum is completely absent. Our calculations show the Stoner spectrum remains weak even at large wave vectors; there is a remnant of spin-rotational invariance even at short wavelength, evidently.

When a proper microscopic exchange matrix element is incorporated into the analysis, one encounters the Green's function defined in Eq. (6). Even at $\vec{q}=0$, we shall realize the structure in the Stoner region, since considerations of spin-rotational invariance place no restraint on this function. A consequence is that even in this limit, one has contributions from Stoner excitations. We shall see that for wave-vector transfers such as those realized in SPEELS experiments found in the literature, the Stoner bands appear prominently.

We conclude this section with a discussion of the explicit form of the exchange matrix element. We proceed as follows. We imagine a large crystal of volume V, with periodic boundary conditions applied to all quantities. Thus, for the electron-electron interactions, we write

$$v(\vec{x}-\vec{y})=\frac{1}{V}\sum_{\vec{Q}} v(\vec{Q})e^{i\vec{Q}\cdot(\vec{x}-\vec{y})}. \tag{10}$$

Then

$$V_{\rm ex}(n\vec{k}\uparrow,\vec{p}_i,\vec{p}_f,m\vec{k}+\vec{q}\downarrow)=\frac{1}{V}\sum_{\vec{Q}} v(\vec{Q})F_{n\vec{k}\uparrow}(\vec{P}_f+\vec{Q}) \times F^*_{m\vec{k}+\vec{q}\downarrow}(\vec{P}_i+\vec{Q}), \tag{11}$$

where

$$F_{n\vec{k}\sigma}(\vec{q})=\int d^3x e^{-i\vec{q}\cdot\vec{x}}\Psi_{n\vec{k}\sigma}(\vec{x}). \tag{12}$$

Use of the form in Eq. (1) allows us to write

$$F_{n\vec{k}\sigma}(\vec{q})=\frac{1}{\sqrt{N}}\left(\sum_{\vec{R}} e^{-i(\vec{q}-\vec{k})\cdot\vec{R}}\right)\sum_{\mu} a_\mu(n\vec{k}\sigma)f_\mu(\vec{q}), \tag{13}$$

where

$$f_\mu(\vec{q})=\int d^3x e^{-i\vec{q}\cdot\vec{x}}\phi_\mu(\vec{x}). \tag{14}$$

The sum over $\vec{R}$ in Eq. (13) may be carried out to give us

$$F_{n\vec{k}\sigma}(\vec{q})=\sqrt{N}\sum_{\vec{G}}\delta_{\vec{q},\vec{k}+\vec{G}}\sum_{\mu} a_\mu(n\vec{k}\sigma)f_\mu(\vec{k}+\vec{G}). \tag{15}$$

If V_i is the volume of the unit cell, then we find

$$V_{\rm ex}(n\vec{k}\uparrow,\vec{p}_i,\vec{p}_f,m\vec{k}+\vec{q}\downarrow) =\sum_{\mu\nu} a^*_\mu(n\vec{k}\uparrow)a_\nu(m\vec{k}+\vec{q}\downarrow) \times\sum_{G} v(\vec{k}-\vec{p}_f+\vec{G})f^*_\mu(\vec{k}+\vec{G})f_\nu(\vec{k}+\vec{q}+\vec{G}). \tag{16}$$

As discussed earlier, the coefficients $a_\mu(n\vec{k}\sigma)$ are provided self-consistently from the multiband generalization of Hubbard model with the hopping integrals given by the Slater-Koster empirical band-structure scheme. We need the explicit form of the orbitals to generate the form factors $f_\mu(\vec{q})$. We discuss our choices below.

We conclude this section by discussing the appropriate form for $v(\vec{Q})$, the matrix element of the electron-electron interaction.

Since the electrons interact inside the metal, quite clearly the interaction will be screened. If we were to describe the screening within the framework of the random-phase approximation, the relevant diagrams are illustrated in Fig. 1(b). The bare Coulomb interaction of Fig. 1(a) should be replaced by the screened form, as illustrated.

A full account of the screening, within the framework of our multiband picture is a formidable undertaking. However, for the exchange scattering process of interest here, we argue screening effects are very modest and may be ignored. Note that the frequency argument of each bubble in Fig. 1(b) is $(\epsilon_a-\epsilon_b)$. We have in mind beam electrons (energy ϵ_a) at least several electron volts above the vacuum level, while the final-state electron created in the excitation process (energy ϵ_b) resides within the $3d$ band complex of the substrate, 5–10 eV below the vacuum level. The wave-vector and frequency-dependent dielectric response function involved in the screening is thus evaluated at a frequency well above the plasma frequency. In addition, the wave-vector transfer involved in the exchange scattering event is substantial, the order of 10^8 cm^{-1} or higher. We may thus safely ignore screening, and use the bare Coulomb interaction in the analysis. Thus, we choose $v(\vec{Q})=4\pi e^2/Q^2$.

The next subsection is devoted to our means of generating the Green's function defined in Eq. (6). As remarked earlier, the random-phase approximation (RPA) will provide the basis for our analysis. We note that in our earlier study, the RPA provides values for the spin-wave exchange stiffness in

excellent accord with experimental data on bulk Fe, and a large wave vectors, it accounted nicely for the features reported in Ref. 2.

B. RPA solution

To proceed, we define an auxiliary two-particle Green's function

$$G_2(nm,\vec{k}\vec{q}\vec{p}_i;\tau)=-\langle T_\tau\{c^+(n\vec{k}\uparrow;\tau)c(m\vec{k}+\vec{q}\downarrow;\tau) \times R^-(-\vec{q},\vec{p}_i;0)\}\rangle. \quad (17)$$

We may generate an equation of motion for this function, and decouple the resulting form within the RPA scheme. The procedure is very similar to that described in Ref. 1. After the decoupling procedure, we find the auxiliary function defined in Eq. (17) obeys the integral equation

$$G_2(nm,\vec{k}\vec{q}\vec{p}_i;i\omega_\nu)=\frac{f(n\vec{k}\uparrow)-f(m\vec{k}+\vec{q}\downarrow)}{i\omega_\nu-\epsilon(m\vec{k}+\vec{q}\downarrow)+\epsilon(n\vec{k}\uparrow)} \times\Bigg\{V(m\vec{k}+\vec{q}\downarrow,\vec{p}_f,\vec{p}_i,n\vec{k}\uparrow) - \sum_{n_1n_2\vec{k}} U(m\vec{k}+\vec{q}\downarrow,n_1\vec{p}\uparrow,n_2\vec{p} +\vec{q}\downarrow,n\vec{k}\uparrow)G_2(n_1n_2,\vec{p}\vec{q}\vec{p}_i;i\omega_\nu)\Bigg\}. \quad (18)$$

In this expression $\epsilon(n\vec{k}\uparrow)$ and $\epsilon(n\vec{k}\downarrow)$ are the energies of up- and down-spin electrons in the ground-state energy bands, and $f(n\vec{k}\uparrow)$, $f(n\vec{k}\downarrow)$ are the associated Fermi-Dirac functions.

In Eq. (18), we have a Bethe-Salpeter equation, which describes the repeated scattering of the excited down-spin electron $(m\vec{k}+\vec{q}\downarrow)$ against the up-spin hole $(n\vec{k}\uparrow)$ produced in the excitation event depicted in Fig. 1(a). The quantity $U(m\vec{k}+\vec{q}\downarrow,n_1\vec{p}\uparrow,n_2\vec{p}+\vec{q}\downarrow,n\vec{k}\uparrow)$ is the matrix element of the Coulomb interaction responsible for this scattering. This is provided by our multiband generalization of the Hubbard model, as given in Ref. 1.

We transform the various quantities which enter the analysis to a representation labeled by the symmetry indices (μ,ν) of the d electron orbitals. For example, we introduce

$$G_2(\mu\nu,\vec{q}\vec{p}_i;i\omega_\nu) \equiv\frac{1}{N}\sum_{nm\vec{k}} a^*_\mu(n\vec{k}\uparrow)a_\nu(n\vec{k}+\vec{q}\downarrow)G_2(nm,\vec{k}\vec{q}\vec{p}_i;i\omega_\nu). \quad (19)$$

The analysis may then be phrased entirely in terms of an ''exchange scattering response function'' $\chi(\mu\nu,\mu'\nu';\vec{q}\omega)$ which, in the basis set provided by the atomic orbitals, may be expressed as follows:

$$\boldsymbol{\chi}(\vec{q},\omega)=\boldsymbol{\chi}_0^{(1,1)}(\vec{q},\omega)-\boldsymbol{\chi}_0^{(1,0)}(\vec{q},\omega) \times\mathbf{U}[\mathbf{1}+\boldsymbol{\chi}_0^{(0,0)}(\vec{q},\omega)\mathbf{U}]^{-1}\boldsymbol{\chi}_0^{(0,1)}(\vec{q},\omega), \quad (20)$$

where the multiplication in Eq. (20) has the character of matrix multiplications in the space (μ,ν) of $3d$ orbital symmetry labels. To derive Eq. (20), one expresses all quantities in Eq. (18) in the orbital basis, and carries out the formal solution in terms of matrix multiplication. A key to one's ability to achieve this solution is our assumption that the $3d$ electrons interact only when they reside on the same lattice site. The kernel in Eq. (18) is then separable. In Eq. (20), the various quantities that enter are

$$\chi_0^{(M,N)}(\mu\nu,\mu'\nu';\vec{q}\omega) =\frac{1}{N}\sum_{nm\vec{k}}\frac{f_{n\vec{k}\uparrow}-f_{m\vec{k}+\vec{q}\downarrow}}{\omega-\epsilon_{m\vec{k}+\vec{q}\downarrow}+\epsilon_{n\vec{k}\uparrow}+i\eta} \times[F_{\mu\nu}(\vec{k},\vec{q},\vec{p}_f)]^M a^*_\mu(n\vec{k}\uparrow)a_\nu(m\vec{k}+\vec{q}\downarrow) \times a^*_{\mu'}(m\vec{k}+\vec{q}\downarrow)a_{\nu'}(n\vec{k}\uparrow)[F^*_{\nu'\mu'}(\vec{k},\vec{q},\vec{p}_f)]^N. \quad (21)$$

Here, $F_{\mu\nu}(\vec{k},\vec{q},\vec{p}_f)$ is an exchange matrix element form factor, defined as

$$F_{\mu\nu}(\vec{k},\vec{q},\vec{p}_f)=\sum_{\vec{G}} v(\vec{k}-\vec{p}_f+\vec{G})f^*_\mu(\vec{k}+\vec{G})f_\nu(\vec{k}+\vec{q}+\vec{G}). \quad (22)$$

In Sec. III, we present numerical results based on the formalism presented in this section, and we discuss the physical content of the various contributions to Eq. (20), which is the central result of the present paper.

III. RESULTS AND DISCUSSION

As just remarked, Eq. (20) contains the central result of the present paper. Formally, the response function described by this equation is structurally rather similar to the dynamic transverse susceptibility studied earlier. However, as we have remarked earlier, the explicit appearance of the exchange matrix element plays a crucial role in the results that follow, by breaking down the strong influence of spin-rotation invariance. Before we present the results of our numerical studies, we discuss the content of this equation.

If we were to retain only the first term in Eq. (20) in the analysis, and use this to evaluate the SPEELS cross section in Eq. (7), then we would be describing the exchange scattering event depicted in Fig. 1(a). The electron and the hole created in the SPEELS excitation process are regarded as freely propagating noninteracting entities at this level of approximation. In the literature, it is commonly assumed that one may interpret SPEELS data within this simple scheme.[13]

The second set of terms in Eq. (20) recognize that after the electron-hole pair have been created in the scattering process, in fact they interact with each other. In our RPA scheme, we have retained repeated scatterings between these entities, described by the ladder graph diagrams of many-body theory.

The interaction between the particle and hole influences the SPEELS spectrum in a qualitative manner. Such final-

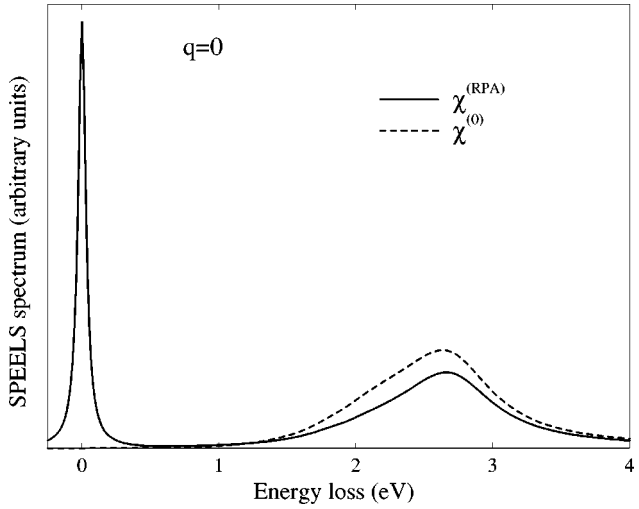

FIG. 2. The solid line shows the SPEELS spectrum calculated with the exchange response function described by Eq. (20). The dashed line is the spectrum at $\vec{q}=0$ provided by the first term only, in Eq. (20). We see the particle-hole interactions shift oscillator strength from the Stoner excitation region near 2.5 eV, down to the spin wave at zero frequency.

state interactions are responsible for the spin-wave loss feature in the SPEELS spectrum for example. For a fixed value of the wave vector $\vec{q}$, the spin-wave excitation appears as a pole in the denominator $[\mathbf{1}+\boldsymbol{\chi}_0^{(0,0)}(\vec{q},\omega)\mathbf{U}]^{-1}$ which lie very close to the real axis in the complex ω plane. These poles lie close to, but not on the real axis, because in itinerant electron magnets, the spin waves are Landau damped: they have a finite lifetime, since they may decay to particle-hole pairs. In the transverse dynamic susceptibility studied in Ref. 1, the same spin-wave poles enter. There we demonstrated that we obtain an excellent account of the spin-wave dynamics of bulk Fe with our model, including an account of the short-wavelength features studied in Ref. 2.

The dynamic transverse susceptibility $\chi_{+-}(\vec{q},\omega)$ may be expressed in a form quite identical to Eq. (20), except in $\chi_0^{(M,N)}$ we find orbital form factors in place of the exchange matrix elements described by $F_{\mu\nu}$ in the present discussion. As remarked above, a general theorem based on spin-rotation invariance of the underlying Hamiltonian enters importantly in the analysis of $\chi_{+-}(\vec{q},\omega)$. This theorem states that as $\vec{q}\rightarrow 0$, the only contribution to $\chi_{+-}(\vec{q},\omega)$ is that from the spin-wave pole, which in this limit is at $\omega\equiv 0$. In the Stoner region, the first term in the analog of Eq. (20) is cancelled precisely by the second term. This theorem is exact in the limit $\vec{q}\rightarrow 0$, and is obeyed by our approximate theory based on the RPA. The calculation reported in Ref. 1 show that even at large wave vectors $\vec{q}$, the Stoner structure is very weak indeed. The response function in Eq. (20), however, has no constraints placed on it even at $\vec{q}=0$ by such considerations.

We illustrate this in Fig. 2, where for $\vec{q}=0$ the solid line shows the spectral density associated with the exchange response function in Eq. (20). To evaluate the exchange matrix elements, we have used radial orbitals discussed below. One sees a prominent spin-wave peak, centered at zero frequency. At the same time, we see a broad feature centered around 2.5 eV, which is the average exchange splitting present in ferromagnetic iron. These are the Stoner excitations, which ''activated'' in the exchange response function, for the reasons just discussed. Our earlier studies of the dynamic transverse susceptibility showed that at small wave vectors, the Stoner feature was absent entirely. The dotted line in Fig. 2 is just the spectral density associated with the first term in Eq. (20). Recall this is the spectrum associated with noninteracting electron-hole pairs. We see that the final-state particle-hole interactions do not shift the maximum of this feature. Clearly, one sees that when the interactions are incorporated, oscillator strength is transferred from the Stoner feature, to the collective spin-wave excitation. The origin of the width of this structure is interesting. At $\vec{q}=0$ we have only vertical transitions which contribute to the Stoner spectrum. Thus the width has its origin in the wave-vector dependence of the exchange splitting.

In the calculations just described, and those reported below, we have employed a finite value of the parameter η in the energy denominator in Eq. (21). At $\vec{q}=0$, the spin-wave feature in the spectral density should be a Dirac δ function, suitably weighted, at zero frequency. The width of the spin-wave feature in Fig. 2 has its origin in our use of a finite value of η. We have chosen $\eta=35$ meV, in this particular case.

As remarked earlier, we find that the SPEELS spectrum is quite sensitive to the radial wave function $R_2(\rho)$ in Eq. (2). Of primary interest to us is the strength of the spin-wave feature, relative to the Stoner spectrum. We wish here to asses the relative strength of the spin-wave loss peak, as a guide to future experiments.

We illustrate this point in Fig. 3, where we present a series of theoretical SPEELS spectra, for the choice

$$R_2(\rho)=\sqrt{\frac{8\alpha^7}{45}}\,\rho^2 e^{-\alpha\rho}. \tag{23}$$

and several values of α. This function may be used to represent crudely the wave function of the $3d$ electron in atomic Fe. The wave-vector transfer $\vec{q}$ has been fixed at $\vec{q}=(2\pi/a)(0.325\hat{x}-0.25\hat{z})$ and the angle and energy of the incoming electron beam at $\theta_i=55°$ and $E_i=31.5$ eV, compatible with the SPEELS data in Fe(100) reported in Ref. 9.

For small values of α, say $\alpha=0.5$ bohr^{-1}, we see a Stoner spectrum rather similar to that calculated from the first term of Eq. (20), shown as a dashed line in the topmost panel of the figure. The spin-wave peak is almost completely absent. As α is increased, with the consequence that $R_2(\rho)$ is spatially more compact, we see the spin-wave peak develop quite nicely. By the time we reach rather large values of α, the spin-wave peak is the dominant feature in the calculated loss spectrum, and the Stoner band becomes very weak. We see this in the calculation for $\alpha=4$. In this bottom most panel, we compare the SPEELS spectrum calculated from the exchange response function in Eq. (20), with that provided in a picture where the dynamic susceptibility $\chi_{+-}(\vec{q},\omega)$ controls the spectrum. Even at this rather large value of wave-vector transfer, we see virtually no hint of the Stoner bands, as discussed above.

The trends in Fig. 3 may be understood from the following argument. When α is large, and $R_2(\rho)$ is spatially compact, in the exchange matrix element, the only process which

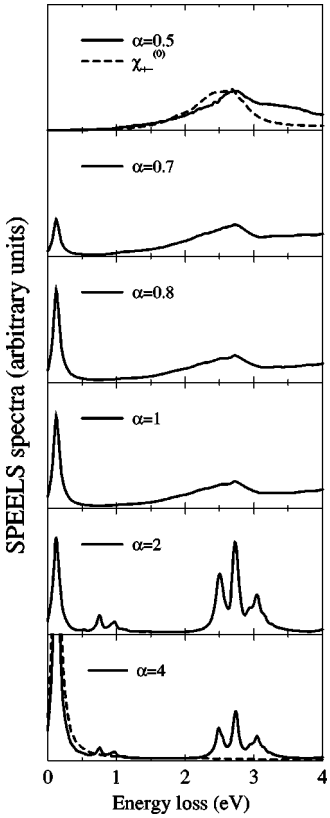

FIG. 3. SPEELS spectra calculated using the atomic radial orbitals given in Eq. (23) for different values of α. The top panel also shows the spectral density of the noninteracting transverse dynamic susceptibility χ^0_{+-} (dotted line). The dotted line in the bottom panel shows the spectral density of the transverse dynamic susceptibility $\chi^{(\mathrm{RPA})}_{+-}$.

contributes significantly is that in which the excitation process is highly localized; the electron and hole are initially localized at the same atomic site. In this limit, the electron and hole interact very strongly, and the spin-wave feature dominates the loss cross section. When α is small, and $R_2(\rho)$ is spatially extended, there is a large probability that in the initial excitation process, the electron and hole are separated considerably. They then interact only weakly, and the calculated spectrum resembles that calculated for noninteracting entities.

Because of the sensitivity of the calculation to the choice of d orbitals, our final set of calculations employ forms of $R_2(\rho)$ generated by electronic structure calculations for bulk Fe. These orbitals were obtained by Pickett *et al.*[10] in the process of reformulating the ''LDA+U'' method for local orbital basis. Their formulation is based on the standard linear combination of atomic orbitals expansion of the Bloch basis functions in which the numerical representation of the atomic orbitals was fit to a sum of Gaussians. The choice of the $3d$ orbitals used in this paper is identical to the $\mathrm{Fe}^0 3d$ orbitals Pickett *et al.*[10] used for Fe in paramagnetic FeO. These are expressed in terms of eight Gaussians

$$R_2(\rho)=\sum_{j=1}^{8} \alpha_j A_j e^{-G_j \rho^2} \tag{24}$$

TABLE I. Expansion coefficients for the Gaussian representation of the $3d$ orbitals of paramagnetic iron, Eq. (24). The coefficients α_j are given in terms of G_j as $\alpha_j = 2048^{0.25} G_j^{1.75}/(\sqrt{3}\pi^{0.75})$. All quantities are in atomic units.

j	G_j	A_j
1	127.0130	0.003946568
2	50.5179	0.01909717
3	20.092900	0.09034960
4	7.991720	0.2971454
5	3.178610	0.5665444
6	1.264260	0.6360391
7	0.502843	0.4632799
8	0.200000	0.3317246

with the expansion coefficients given in Table I. The $\vec{q}=0$ calculation reported in Fig. 2 was carried out with the wave functions just described.

It is of interest to compare the wave functions generated by the electronic structure analysis, with the empirical form in Eq. (23). We do this in Fig. 4, where the radial wave function generated by the full calculation is displayed as the bold, solid line. Its peak lies closer to the nucleus than that with $\alpha=4$. However, the proper solid-state wave function has a long tail that extends well out into the far reaches of the unit cell. Thus, we have a substantial probability of exciting a particle-hole pairs at appreciable separations. (The probability of encountering the electron in a spherical shell of thickness dr is $r^2|R_2(r)|^2 dr$, so the factor of r^2 enhances the importance of relatively large separations.)

In Fig. 5(a), we show a calculated SPEELS spectrum, through use of the wave functions supplied by the electronic structure calculations. The parameter η in the denominator of Eq. (21) has been chosen to be 35 meV. Both the spin-wave loss peak, and the Stoner region appear prominently. Roughly 35% of the integrated strength of the full spectrum resides in the spin-wave feature. The small structures just

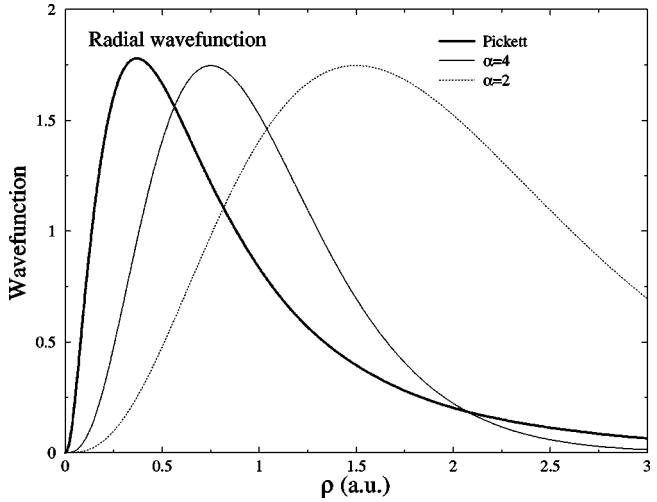

FIG. 4. The radial wave functions used in the SPEELS calculations. The bold line corresponds to the radial orbital generated by electronic structure calculations and the thin lines show the atomiclike orbitals of iron [Eq. (23)] for two different values of parameter α.

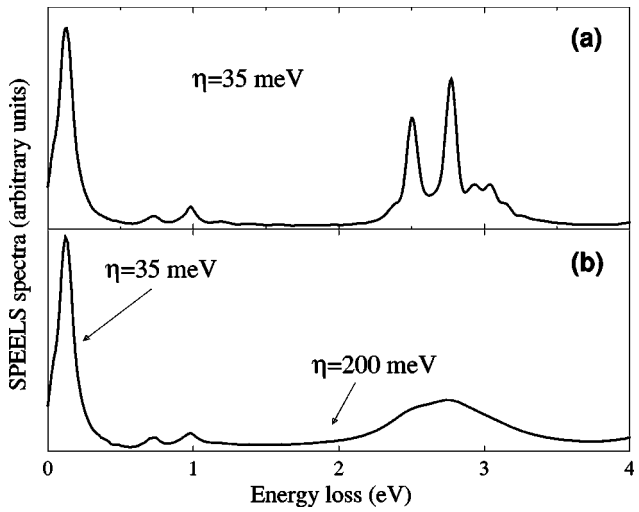

FIG. 5. SPEELS spectra calculated through use of the wave functions generated by electronic structure calculations with (a) $\eta = 35$ meV and (b) $\eta = 35$ meV in the spin-wave region and $\eta = 200$ meV in the Stoner region.

below 1 eV loss energy are produced by low-lying Stoner excitations; we find these structures also in the spectral density of the first term of Eq. (20), which describes the noninteracting electron-hole pair.

We see clear and prominent structure in the Stoner region, in the SPEELS spectrum displayed in Fig. 5(a), while the experimental spectra are rather featureless. Of course, the experiments are carried out on surfaces, under conditions where the electron mean free path is in the range of two or three interatomic spacings. Our calculations apply to bulk Fe. It is the case, however, that the experimental studies of the Stoner region are carried out with rather poor energy resolution, in the range 200–300 meV. In Fig. 5(b), we present a theoretical spectrum where η is retained to be 35 meV in the spin-wave loss regime, but is increased to 200 meV in the Stoner band. By this means, we may simulate the relatively poor resolution employed in these experiments. We see the structure is now washed out, and the theoretical result bears a strong resemblance to the data.

IV. FINAL REMARKS

In this paper, we have presented realistic calculations of the SPEELS spectrum of an electron propagating in the bulk of ferromagnetic Fe. These are based on a realistic electronic structure, and an exchange matrix element generated by a microscopic analysis. For reasons outlined above, use of a proper exchange matrix element is essential, if quantitative results are to be achieved. Past discussions have been based on either greatly oversimplified, schematic models of the electronic structure,[11] or simple density of states arguments[13] which overlook the important role played by final-state interactions between the electron and the hole. Such interactions are essential, since they are responsible for the appearance of the spin-wave loss peak in the SPEELS spectrum.

Our calculations have been undertaken for several reasons. One key issue is the following. As we have discussed, the Stoner region of the SPEELS spectrum has been explored in ''complete'' SPEELS studies which employ both a polarized incident beam, and which utilize spin analysis of the scattered electrons.[3,4,9] In such studies, the spin-flip contribution to the electron-loss spectrum can be isolated. It is our view that the calculations which lead to the prominent spin-wave loss peak in Fig. 5 are quantitatively reliable, and establish that the spin-wave loss peak should be observable, in a suitable experiment. We should remark here that our results possibly suppress the spectral weight of the spin-wave peak somewhat. This is because we use the unscreened Coulomb interaction for the beam electrons, whereas we assume that the interaction between substrate electrons is strongly screened and only on-site Coulomb matrix elements need be considered. The presence of off-site interactions between substrate electrons, as well as some screening for the beam electrons should enhance the correlation between the final-state electron-hole pair, and consequently enhance the spin-wave mode in the SPEELS spectrum. However, we feel these effects should prove to be only minor corrections to the presented results.

While the calculations reported here are for an electron which scatters from spin excitations in bulk Fe, we have shown earlier[1] that standing spin waves appear as clear, well-defined excitations in ultrathin films similar to those employed in past SPEELS experiments. In the film, or at magnetic surfaces, the spin-wave loss feature should appear with intensity, relative to that of the Stoner spectrum, comparable to that found in the present study. We shall direct attention to the SPEELS spectrum of ultrathin films in the future.

One may inquire why the spin-wave loss peak has not been reported in experiments carried out to date. Since the Stoner feature is very broad, all experiments to date have employed rather low resolution, in the range of 300 meV. Under these circumstances, the spin-wave loss feature is obscured by the broad, quasielastic peak always present. In off-specular studies of surface phonons, energy resolution in the range of 3 meV is employed in numerous experiments carried out at higher resolution, as the quasielastic peak is confined to the loss region well below the spin-wave frequency domain. Such an experiment will prove a challenge, since as the energy resolution is improved, the signal that may be realized degrades substantially.[14] It is difficult to envision a ''complete'' experiment with energy resolution in the 3 meV range used in the surface phonon studies, since as discussed earlier, the absolute cross section for exciting spin waves is substantially smaller than that for exciting surface phonons.[5] Also, spin detectors are highly inefficient. We note that it is not necessary to use spin analysis in the final state to observe the spin-wave loss feature, since it resides in a loss regime well above the phonon spectrum.

It would be intriguing to perform an ''on/off'' experiment as follows. As we have seen, if the spin of the beam electron is in the minority-spin direction, the spin-wave loss peak is a prominent feature in the loss spectrum. This feature is completely absent, if the spin of the beam electron is in the majority-spin direction. This is a consequence of angular momentum conservation. Emission of a spin wave decreases the z component of the angular momentum of the substrate spins by $\hbar$. This angular momentum must be transferred to the beam electron. If the beam electron spin is parallel to the minority-spin direction, this is accomplished by the spin flip depicted if Fig. 1(a). The beam electron cannot absorb the

angular momentum if its spin is parallel to the majority-spin direction, as spin-wave emission is not allowed in this case. By using a polarized beam, and comparing the SPEELS spectrum for the case where the beam electron has spin first parallel and then antiparallel to the majority-spin direction in the substrate, one should be able to isolate the spin-wave loss feature, and discriminate against the non-spin-flip background, without detecting the spin of the scattered electron. It is our view that such a study, carried out with most resolution (25–50) meV should be feasible with presently available spectrometers. Such an experiment, if successful, would allow the first access to the short-wavelength collective spin excitations of an important class of materials.

The present analysis provides us with a theoretical base from which another basic question may be explored. This is a quantitative assessment of the energy dependence and magnitude of the spin asymmetry of the electron mean free path in the ferromagnetic metals. The spin-flip scattering processes examined here control the spin asymmetry in the ''hot electron'' mean free path, in the ferromagnetic transition metals. It has been argued that this controls a number of key spin-dependent phenomena; for electron beams used as probes of magnetics surfaces in films, for electrons photoemitted from such materials, and for secondary electrons.[15] However, it is the case that quantitative calculations have shown[16] that spin-dependent elastic scatterings can provide adequate accounts of phenomena that some have argued[17] provide evidence for the presence of spin dependence of the inelastic mean free path. Quantitative calculations of the spin dependence of the inelastic mean free path, as opposed to simple phenomenological models, will provide a basis for assessing the relative importance of these two sources of spin asymmetry in electron propagation. The analyses described in Ref. 1, and the formalism developed in the present paper provide the basis for such a study.

ACKNOWLEDGMENTS

The authors are indebted to Professor Warren E. Pickett, who kindly supplied us with the wave functions employed to generate the results displayed in Figs. 2 and 5. This research was supported by the U.S. Department of Energy, through Grant No. DE EC03-84EB4583 and by NSF Grant No. DMR-97-08499.

[1] H. Tang, M. Plihal, and D. L. Mills, J. Magn. Magn. Mater. **187**, 23 (1998).

[2] T. G. Perring, A. T. Boothroyd, D. McK. Paul, A. D. Taylor, R. Osborn, R. J. Newport, J. A. Blackman, and H. A. Mook, J. Appl. Phys. **69**, 6219 (1991).

[3] D. Venus and J. Kirschner, Phys. Rev. B **37**, 2199 (1988).

[4] D. L. Abraham and H. Hopster, Phys. Rev. Lett. **62**, 1157 (1989).

[5] M. Gokhale, A. Ormeci, and D. L. Mills, Phys. Rev. B **46**, 8978 (1992).

[6] For a review of early pioneering studies, see A. J. Freeman, C. L. Fu, S. Ohnishi, and M. Weinert, in *Polarized Electrons in Surface Physics*, edited by R. Feder (World Scientific, Singapore, 1985), p. 3; a more recent review is given by Ruqian Wu and A. J. Freeman (unpublished).

[7] For example, R. M. White, *Quantum Theory of Magnetism* (McGraw-Hill, New York, 1970), Chaps. 1–3.

[8] J. F. Cooke, J. W. Lynn, and H. L. Davis, Phys. Rev. B **21**, 4118 (1980).

[9] T. G. Walker *et al.*, Phys. Rev. Lett. **69**, 1121 (1992).

[10] W. E. Pickett, S. C. Erwin, and E. C. Ethridge, Phys. Rev. B **58**, 1201 (1998).

[11] G. Vignale and K. S. Singwi, Phys. Rev. B **32**, 2824 (1985).

[12] See, for instance, S. Lehwald, F. Wolf, H. Ibach, Burl M. Hall, and D. L. Mills, Surf. Sci. **192**, 131 (1987).

[13] For example, H. Hopster, in *Ultrathin Magnetic Structures I*, edited by B. Heinrich and J. A. C. Bland (Springer-Verlag, Heidelberg, 1994), p. 123.

[14] H. Ibach and D. L. Mills, *Electron Energy Loss Spectroscopy and Surface Vibrations* (Academic, San Francisco, 1982), Chap. 2.

[15] H. C. Siegmann, in *Selected Topics in Electron Physics*, edited by M. Campbell and H. Kleinpoppen (Plenum, New York, 1996).

[16] M. P. Gokhale and D. L. Mills, Phys. Rev. Lett. **66**, 2251 (1991).

[17] D. P. Pappas *et al.* Phys. Rev. Lett. **66**, 504 (1991).